J Mater Sci: Mater Med (2011) 22:451–460
DOI 10.1007/s10856-011-4233-7

Porous calcium alginate–gelatin interpenetrated matrix and its biomineralization potential

Izabela-Cristina Stancu · Diana Maria Dragusin · Eugeniu Vasile · Roxana Trusca · Iulian Antoniac · Dan Sorin Vasilescu

Received: 3 August 2010 / Accepted: 11 January 2011 / Published online: 30 January 2011

Abstract Artificial bone composites exhibit distinctive features by comparison to natural tissues, due to a lack of self-organization and intimate interaction apatite-matrix. This explains the need of "bio-inspired materials", in which hydroxyapatite grows in contact with self-assembling natural polymers. The present work investigates the function of a rational design in the hydroxyapatite-forming potential of a common biopolymer. Gelatin modified through intrinsic interactions with calcium alginate led through freeze-drying to porous hydrogels, whose architecture, constitutive features and chemistry were investigated with respect to their role on biomineralization. The apatite-forming ability was enhanced by the porosity of the materials, while the presence of alginate-reinforced Gel elastic chains, definitely favored this phenomenon. Depending on the concentration, polysaccharide chains act as "ionic pumps" enhancing the biomineralization. The mineralization-promoting effect of the peptide-polysaccharide network strictly depends on the hydrogels structural, compositional and morphological features derived from the interaction between the above mentioned two components.

I.-C. Stancu (✉) · D. M. Dragusin · D. S. Vasilescu
Polymer Chemistry and Technology, Group of Polymer Physics & BioMaterials, University Politehnica of Bucharest, 149 Calea Victoriei, Sector 1, 010072 Bucharest, Romania
e-mail: izabela.cristina.stancu@gmail.com

E. Vasile · R. Trusca
METAV Research & Development, 31 C.A. Rosetti, Sector 2, Bucharest, Romania

I. Antoniac
Faculty of Materials Science and Engineering, University Politehnica of Bucharest, 313 Splaiul Independentei, Sector 6, 060042 Bucharest, Romania

1 Introduction

Bioactive ceramics such as calcium orthophosphates and especially hydroxyapatite (HA) are suitable as hard tissue (HT) substitutes, mainly due to their capacity to bind to the living bone and teeth [1–7]. However, their poor mechanical and elastic properties decrease their chances to success in load-bearing biomedical applications. It is well known that in naturally calcified tissues, the biopolymers (mainly collagen) are responsible for the superior strength and partial elasticity [3]. Therefore, composite materials have been proposed as an improved solution for overcoming the mechanical limitations of both ceramics and polymers. However, the properties of artificial bone composites have been proved to be very different when compared to natural tissues, probably due to a lack of self-organization and intimate interaction between apatite and the protein matrix [8]. In this circumstance, the need of the so-called "bio-inspired materials", in which HA grows in contact with self-assembling fibers of natural polymers has been emphasized [8].

Thus, polymer materials supporting/enhancing mineral phase formation remains one of the most promising classes of biomaterials for bone repair, or their regeneration [1–3, 8–11]. The main advantage of these materials over classical bone fillers consists in their in situ transformation in polymer-HA bone-like composite. They also present the advantage of HA generation inside the bone tissue, leading to an intimate interaction between HA and the polymer matrix, thus improving the further osteointegration of the implant.

Biomineralization is the general phenomenon by which mineral forms in living organisms. The process is complex, multidisciplinary and presents species-specific features; the physiological/pathologic nature and/or the localization in

the body lead to distinct traits. The literature on the biomimetic mineralization is extremely wide. However, there is still a lack of a functional and controlled method of mineralization induction aimed to HT regeneration. Insufficient understanding of body-mineralization leads to the need of a deeper process analysis. Living organisms are responsible for the synthesis of over 60 types of minerals; among them, calcium orthophosphates are the main mineral constituents of HT [12] under the form of calcium defficitary HA ($Ca_{10-x}(HPO_4)_x(PO_4)_{6-x}(OH)_{2-x}$—CDHA) currently named biologic apatite [13, 14]. There is no consensus over the beginning of the calcification-responsible nucleation. However, the importance of the organic framework is generally recognized [15]. The studied hypotheses/mechanisms have led to several elements deciding the mineralization occurrence and control; the most important ones seem to be: (1) the precipitation of HA from saturated solution at body temperature; (2) the presence of calcium and phosphate ions in the liquid environment; (3) the existence of a permeable organic matrix for mineral support; (4) the existence of selective "*ionic pumps*" attracting calcium and phosphate ions inside the "cages" of the organic scaffold. Different attempts were made to create a biomaterial able to induce a controlled biomimetic mineralization.

The present work is devoted to the investigation of the role of a rational design in the HA-forming potential for a polymer scaffold. This typically starts from the analysis of the target application and tissues. For superior performances the biomaterial is ab initio developed, based on macroscopic (dimensional stability, hydrophilicity, mechanical strength, etc.) and microscopic (porosity, phase segregation, local electrical charge, etc.) characteristics. In this study, a common biopolymer, namely gelatin, was modified through interactions with a linear non-mammal polysaccharide, namely calcium alginate, leading through freeze-drying to porous interconnected hydrogels, whose architecture, constitutive features and chemistry were investigated with respect to their role in the mineralization occurrence. The proposed hydrogels are extremely simple, but provide important findings regarding the importance of the synergetic effect of the above mentioned factors, namely architecture, chemistry and structure. Despite its effortlessness, the model is justified through its further functioning and convenience.

2 Materials and methods

2.1 Materials

Gelatin B (Gel) (cell culture tested) obtained by the alkaline treatment of bovine collagen was supplied from Sigma-Aldrich. Pharmaceutical grade, low viscosity sodium alginate (SA) rich in α-L-guluronic residues (approx. 70% of G-block content) was purchased from Medipol SA (Lausanne, Switzerland). Glutar-aldehyde (GA) was supplied from Sigma-Aldrich as 25% solution in water. Calcium chloride—$CaCl_2(2H_2O)$ and sodium azide—NaN_3 were supplied from Sigma-Aldrich and used as received.

All the salts needed to prepare the simulated body fluid (SBF) (sodium chloride (NaCl), sodium hydrogen carbonate ($NaHCO_3$), potassium chloride (KCl), di-potassium hydrogen phosphate trihydrate ($K_2HPO_4{\cdot}3H_2O$), magnesium chloride hexahydrate ($MgCl_2{\cdot}6H_2O$), calcium chloride ($CaCl_2$), sodium sulfate (Na_2SO_4)) were supplied from Sigma-Aldrich and used as received. Distilled water was used as solvent. Hydrochloric acid 1 N was supplied by CHIMOPAR Bucharest. TRIS (tris-hydroxymethyl aminomethane) supplied from Sigma-Aldrich, 99+% was used so that to maintain the pH at 7.4.

Bicinchoninic Acid (BCA) kit for protein determination was purchased from Sigma-Aldrich and used as such. The kit contained reagent A: BCA solution and reagent B: 4%(w/v) $CuSO_4{\cdot}5H_2O$ solution.

2.2 Scaffolds

Gel aqueous solution (20% wt) was prepared by the dissolution of the protein in distilled water, at 40°C; NaN_3 (0.1 wt%) was used to prevent bacterial growth. SA solution (4 wt%) was prepared by the dissolution of the polysaccharide in distilled water at room temperature, under vigorous stirring. Gel-SA mixtures with increasing content of SA were obtained by mixing the previously described solutions, under a powerful stirring, at 40°C; different ratios have been used (see Table 1).

Following the homogenization of the resulting solution, GA was added to crosslink 25% of the amino groups from Gel. The crosslinking agent was added dropwise, and diluted with distilled water, in order to avoid a preferential local crosslinking. Thus, the final Gel-SA compositions contain constant amount of crosslinked Gel and increasing SA amounts.

Table 1 Composition of the initial mixtures used to prepare the raw materials

Sample	Gel:SA (wt:wt)
A1	100:2
B1	100:4
C1	100:8
D1	100:10

All samples had 100 ml

Subsequently, the mixtures were poured into Petri dishes and cooled down to 4°C. After the hydrogels have hardened, they have been removed from the Petri dishes and have been immersed in aqueous $CaCl_2$ solution (five times excess with respect to the carboxyl groups) for the crosslinking of the SA, for 24 h. The non-reacted $CaCl_2$ has been extensively removed by water-extraction.

After the crosslinking treatment, hydrogels cylinders with 10^{-2} m diameter and 1.5×10^{-2} m height, have been cut, washed and lyophilized for 24 h, under vacuum (0.47–0.52 mbarr) at −50°C. For the lyophilization a Labconco (FreeZone 2.5) device was used. For simplicity, the resulted materials are denoted as A2, B2, C2, D2 respectively.

3 Characterization of the scaffolds

3.1 Falling ball viscometry

The interactions between SA and Gel have been investigated through the evaluation of the dynamic viscosity of the Gel-SA mixtures using a Falling Ball Viscosimeter KF10 (RheoTec Messtechnik GmbH, Otterdorf-Okrilla, Germany). Measurements have been performed at 35–55°C and the dynamic viscosities have been calculated using the well known equation:

$$\eta = t(\rho_1 - \rho_2)KF \quad (1)$$

where η represents the dynamic viscosity (mPas), t the travelling time of the ball (s), ρ_1 the density of the ball according to the test certificate (g/cm^3), ρ_2 the density of the measuring substance (g/cm^3), K the ball constant according to the test certificate (mPas cm^3/g), F the working angle constant.

3.2 Crosslinking efficiency

3.2.1 GA-crosslinking of Gel

The first investigation of the success of the crosslinking of the Gel has been performed through the quantitative detection of the Gel released during the $CaCl_2$ treatment of the scaffolds. Secondly, the Gel release from the hydrogel cylinders has been investigated during 3 weeks, at 36.5°C, in distilled water. Samples have been analyzed after 7, 10, 13, 16, 19 and 21 days, respectively. All tests have been performed using the BCA method, consisting in the BCA treatment of the solutions supposed to contain the peptide. The method is based on the proteins' property of reducing alkaline Cu(II)–Cu(I) in a concentration-dependent manner. BCA is a highly specific chromogenic reagent for Cu(I), forming a purple complex specifically absorbing at 562 nm. The absorbance is directly proportional to the protein concentration. The BCA working reagent was prepared in accordance with the protocol described by the producer, as 50 parts reagent A + 1 part reagent B. A volume of 0.1×10^{-3} l sample was mixed with 2×10^{-3} l working reagent directly in the UV–VIS cells; the resulting solution was incubated at 37°C and measured after 30 min at 562 nm. A CINTRA 101 double-beam UV–VIS spectrometer has been used under the fixed wavelength evaluation mode. The concentration of the released Gel was estimated from a calibration curve obtained using Gel solutions of known concentration in the range of 0–2 mg/ml; the amount of released peptide (non-crosslinked) was thus obtained. Measurements were performed in triplicate, showing a good reproducibility.

3.2.2 $CaCl_2$-crosslinking of SA

The success of the SA crosslinking has been estimated gravimetrically. Briefly, the hydrogels submitted to the above described non-crosslinked Gel extraction in distilled water have been dried and weighed before and after the peptide detection experiment. If the SA crosslinking was not efficient, residual SA should remain into the scaffold; since SA is hydrosoluble it should be released during water immersion. The mass loss due to SA release during the peptide extraction was calculated as follows:

$$w_{SA} = w_0 - w_f - w_{\text{Gel}}, \quad (2)$$

where w_{SA} is the mass of residual SA, w_0 and w_f are the initial, respectively the final masses of the dried hydrogel cylinders and w_{Gel} is the mass of released Gel as it results from the previously described BCA method. Measurements were also carried out in triplicate.

3.3 Porosity examination

Morphological information with respect to the porosity, pores' interconnection and other features has been obtained through the SEM analysis of the gold-coated liophylized hydrogel cylinders. The analysis has been performed using a QUANTA INSPECT F SEM device equiped with a field emission gun (FEG) with a resolution of 1.2 nm and with an X-ray energy dispersive spectrometer (EDS).

3.4 Swelling ability

The swelling assessment was performed as follows: the A2-D2 hydrogel cylinders were dried weighed (to record the dry weight—w_d) after the extraction of unreacted biopolymers and then immersed in distilled water to explore their maximum swelling degree (MSD). The swelling behavior was assessed using the blot-and-weight method.

All scaffolds were allowed to swell at constant temperature (36.5°C) until constant mass was achieved (w_w). MSD was calculated as:

$$\mathrm{MSD} = (\mathrm{w_w} - \mathrm{w_d})/\mathrm{w_d} * 100 \quad (3)$$

Experiments were performed in triplicate for all polymer series.

3.5 In vitro mineralization ability testing

The capacity of the A–D Gel-SA scaffolds to induce HA formation has been explored through the incubation of the cylinders in a SBF solution, miming the ionic composition of the human plasma. The preparation of the SBF was performed as recommended by Kokubo for the revised-SBF formulation [16].

The polymer samples have been immersed in distilled water to reach their MSD prior to incubation in SBF. Thereafter they have been introduced in 50 ml of freshly prepared SBF, at 36.5°C, for 3 weeks. The SBF was changed every 3 days. After 3 weeks, the samples were removed from the beakers and kept in a large excess of distilled water used to remove the residual salts physically deposited onto the samples. Washing has been carried out for 24 h and then the materials have been dried at 40°C to constant mass.

The evaluation of the in vitro mineralization ability has been performed through SEM and Fourier transformed infrared spectroscopy (FT-IR). The FT-IR spectra were taken on a Jasco 6200 spectrometer equipped with a Specac Golden Gate attenuated total reflectance (ATR) accessory, using a resolution of 4 cm^{-1} and an accumulation of 60 spectra, in the 4000-400 cm^{-1} wave number region.

4 Results and discussion

The synthesized hydrogels consist in insoluble interpenetrated crosslinked Gel and calcium alginate (CA). The materials were prepared using identical Gel content and increasing SA per constant volume of distilled water. This has led to materials with different characteristics that are further discussed. The idea of this study was to prove that the rational design of biopolymer scaffolds in terms of 3D porous architecture and chemical functionality of the insoluble organic framework could be useful for inducing the occurrence of a biomimetic mineralization. In this aim, the first part of this work has been devoted to the analysis of structural and morphological aspects of the scaffolds. The second part presents the results of the in vitro mineral formation ability test and a relationship between morpho-structural features and the induction of calcification.

4.1 Characterization of the hydrogels

Since during the preparative step, an important increase of the viscosity of each Gel-SA solution has been noticed after the mixing of the two biopolymer components, a viscometry study was a compulsory step. The results are presented in Fig. 1.

The highest increase of the viscosity has been noticed for sample D1, when the synergetic effect has been noticed as the strongest one. It is followed by C1, B1 and A1. The viscosities of A1–C1 are inferior to the viscosity characteristic to the Gel solution, while the viscosity of D1 is slightly higher than that of Gel. At the same time, the differences between the dynamic viscosities of A1 and B1 against the one of Gel are significant, while C1 and D1 present similar dynamic viscosities to those typical for Gel.

Therefore it can be concluded that strong interactions occur between Gel and SA in each corresponding Gel-SA mixtures. Moreover, stronger interactions have been noticed for C1 and D1, when compared to the results recorded for A1 and B1. Nevertheless, the results have shown that the intensity of this interaction was, as expected, increasing with the SA content, suggesting that the polysaccharide is most likely responsible for a physical strengthening of the resulting polymer gel. This fact might be explained through the occurrence of intense physical intermolecular interactions between the peptide and the polysaccharide macromolecules, since both biopolymers are hydrosoluble and present specific functionalities (Gel contains $–NH_2$, –COOH, –OH while SA has $–COO^-$ and –OH); these interactions are proportional with the increase of the alginate content.

All the obtained Gel-SA mixtures were homogeneous and rather viscous. In order to obtain a completely water-insoluble polymeric material to serve as framework for the mineralization study, a two steps crosslinking procedure has been applied. The in situ crosslinking of Gel with GA has been performed as the first step since the Gel is hydrosoluble and it might have been lost during the $CaCl_2$ treatment of SA. This GA-Gel crosslinking has preserved the important thermosensitive character of the peptide component. Thus, the resulting mixtures were viscous fluids at above 35°C, while after cooling down to 4°C strong transparent gels very easily to handle have been obtained. Therefore, the resulted hard hydrogels have been submitted to the second crosslinking process that has occurred by the diffusion of $CaCl_2$ into the water-swelled scaffolds. The diffusion of the crosslinking agent has been favored by the high water content of the materials. The success of the crosslinking of Gel has been proved in two steps: (a) the Gel release into the $CaCl_2$ solution during the SA crosslinking has been monitored through UV-VIS spectrometry, using the BCA protein detection method and

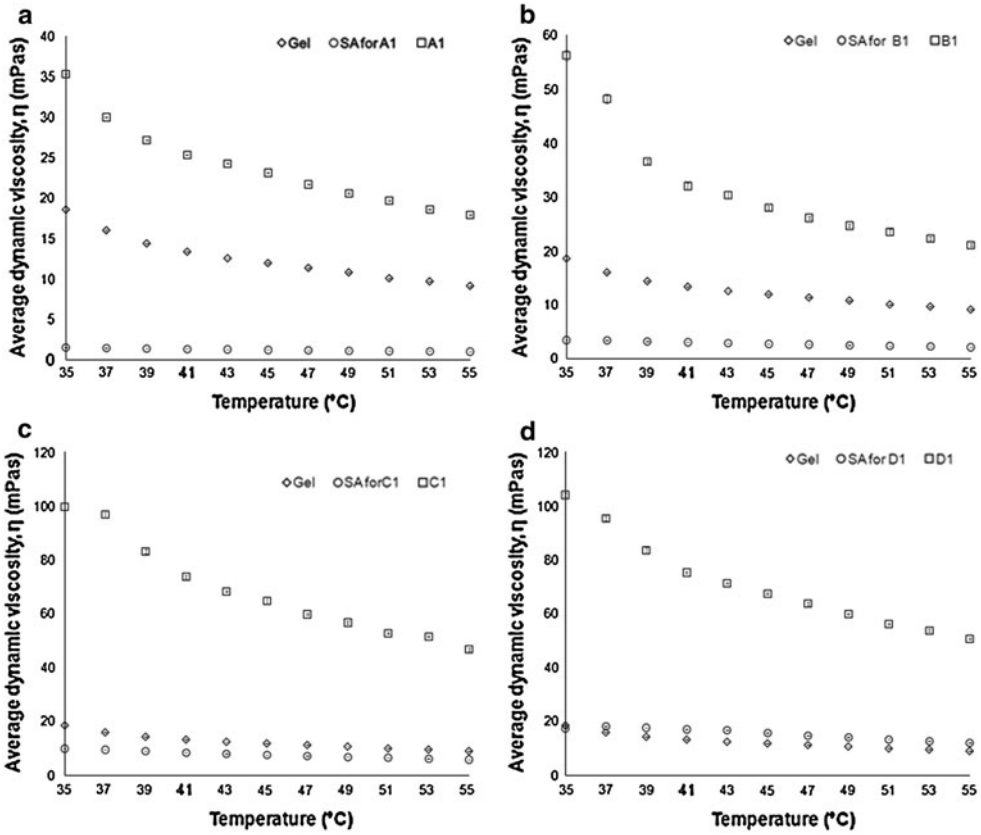

Fig. 1 Dynamic viscosities against temperature for various compositions: **a**–**d** A1–D1 against the corresponding simple SA and Gel solutions

the results indicated that no free Gel has been detected. This means that no Gel has been released, as non-crosslinked, from the GA-treated Gel-SA mixtures. Secondly, the stability testing of the Gel from the final A2-D2 hydrogels in distilled water, at 36.5°C has indicated that only a very slight amount of peptide has been released (see Fig. 2). The values of the Gel loss (calculated as the ratio between the mass of total Gel released from samples A2–D2 during the test, and the initial Gel mass in samples A2–D2, %) range between 0–0.36% for A2, 0–0.35% for B2, 0–0.33% for C2 and 0–0.3% for D2, with STDV $< \pm 0.009$. These results correspond to strongly crosslinked samples, with crosslinking degrees around 99.7% (estimation based on the mass loss with respect to the initial mass of the sample), confirming the stability of the Gel into the synthesized materials. The low standard deviations noticed in the graph suggest a homogeneous behavior of all the studied compositions. Figure 2 states that the Gel-release stops after 13 days.

The gravimetric investigation of the dried scaffolds A2-D2 before and after the Gel-stability test has suggested the insolubility of the polysaccharide component stating for the successful crosslinking of the SA. No extra mass loss (w_{SA}) has been evidenced (using Eq. 2), except for the one due to the Gel release (w_{Gel}). It was proved that the mass loss is not due to any residual $CaCl_2$ since the presence of Ca ions has been revealed through X-ray microanalysis of the materials, while Cl^- ion has not been detected. This proves

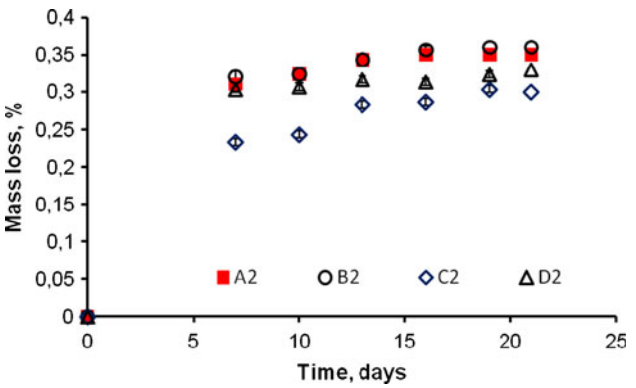

Fig. 2 The evolution of the Gel loss in samples A2–D2 (average for three samples), as resulted from the free Gel released during the 3 weeks peptide-crosslinking efficiency test

that CA has been efficiently formed and no free SA was released during the 21 days of the samples immersion in distilled water. This does not mean that all the sodium carboxylate groups from the SA have been converted to calcium carboxylate. The CA present both types of carboxylate functions but the formation of Ca^{2+} crosslinks leads to the insolubility of the matrix. This is in agreement with the CA content-dependent evolution of the MSD as it will be later emphasized.

These findings are very important both with respect to the composition of the scaffolds, but also because the

materials were further subjected to the testing of the mineralization potential through immersion into an aqueous SBF solution. These data imply that the samples A2–D2 are stable while immersed in SBF for the whole duration of the mineralization evaluation.

The study has been further continued with the analysis of the samples' micro-architecture with respect to the porosity and the interconnected character of the pores. SEM morphological investigation of the freeze-dried samples A2-D2 before the incubation in SBF has shown porous structures with interconnected pores, as displayed in Figs. 3 and 4.

The porosity of the dried samples ranges from micro- (>1 μm) to macro-porosity (in the range of 300–600 μm). The pores are non-homogeneous in shape and size. The pores are columnar to the edge and more spherical at the center of the materials (see Fig. 4).

The size of the pores is decreasing with increasing the amount of polysaccharide, from an average value of approximately 300 μm in A2 and B2 to an average value of approximately 150 μm in C2 and D2.

Quite interesting, the porosities of samples A2 and B2 are very similar (panels a and b in Fig. 3). The same likeness was noticed when comparing samples C2 and D2 (panels c and d in Fig. 3). However, significant differences appear between the two groups: beside the dimension of the pores, it can be seen that increasing the CA amount in the scaffold leads to the augmentation of the thickness of the separation walls between the pores (see Fig. 3).

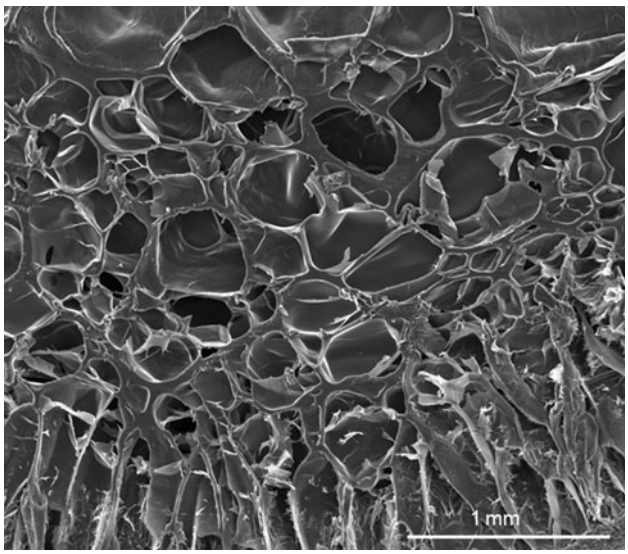

Fig. 4 Cross-section showing the difference in the pores' shape, from the edge to the center, for sample C2

This effect is consistent with the results obtained from the viscometric investigation of the Gel-SA interaction in samples A1–D1. Thus, the increasing SA content in the original mixtures corresponds to increasing CA content in samples A2-D2.

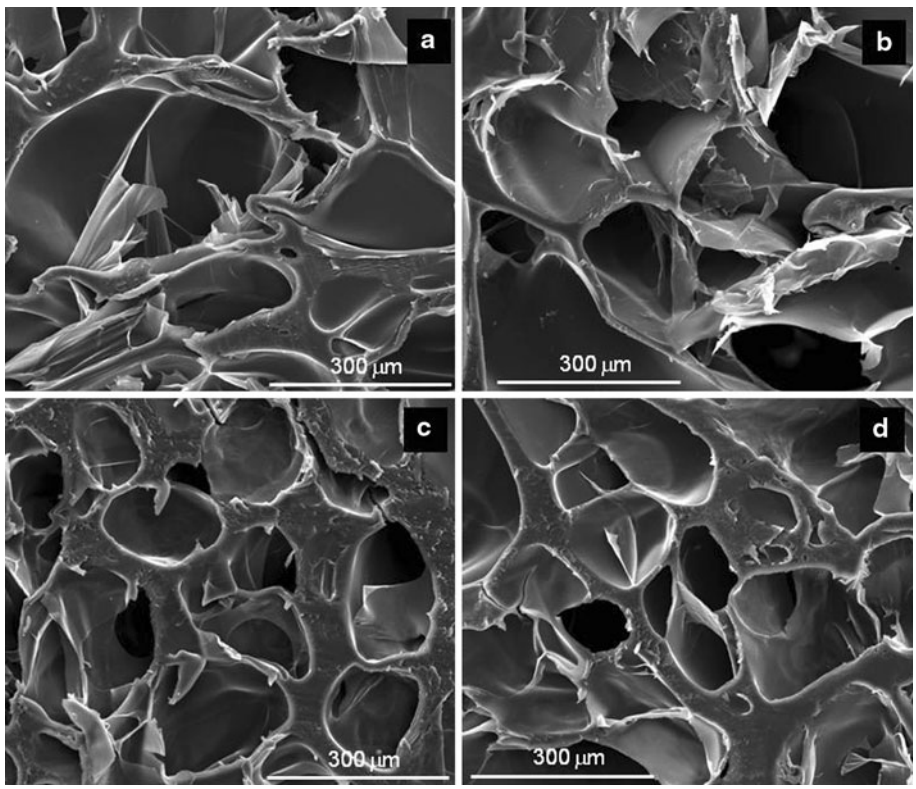

Fig. 3 SEM images displaying the porosity and the interconnectivity of the pores (as obtained from the analysis of cross-sections) of the freeze-dried materials: **a** A2, **b** B2, **c** C2, **d** D2. The dimension of the pores is decreasing while the thickness of the separation walls in increasing from A2 to D2

Moreover, the stronger the interaction between Gel and SA corresponds to stronger connection between Gel and CA in the final hydrogels. These findings are in accordance with the results obtained for the water affinity, expressed as MSD in Fig. 5. Since the samples do contain the same ratio of Gel, the swelling of the A2–D2 scaffolds directly increases with the CA content. Moreover, according to the MSD values, the scaffolds may be divided into two groups: samples A2 and B2 with MSD in the range of 400–550% and samples C2 and D2 with MSD in the range of 650–800%. As may be seen from Fig. 5, the samples containing high alginate percentage are characterized by a superior swelling index, considering that all the materials present the same crosslinking degree of the polysaccharide. The explanation probably consists in a higher hydrophilicity of the alginate.

4.2 In vitro mineralization capacity

Before any other test we have routinely checked the lack of precipitation during the incubation period inside the testing vessel.

The mineralization capacity of the A2–D2 hydrogels was first explored through SEM investigation of eventual mineral deposits made (onto the surface of the samples), during the incubation in SBF.

None of the hydrogels was coated by uniformous mineral layer at the end of the incubation time. Nevertheless, all the hydrogels have presented mineral phase nucleation areas of, homogeneously distributed onto the polymer surfaces. The constitutive nuclei are small globules (elementary features of approximately 50 nm, difficult to measure since they tend to agglomerate); in turn, these agglomerates lead to small mineral islets at micronic (maximum 5 μm length) and under-micronic scale, entraped into the polymers.

Extensive mineral deposits were detected exclusively on hydrogels A2 and B2. They appeared as thick non-homogeneously structures spread onto the polymer scaffolds. These mineral features are organized in elementary tablets as it can be seen in the internal part of the deposits (Fig. 6).

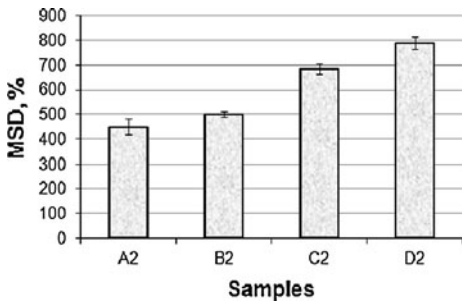

Fig. 5 The dependence of the average values of the MSD determined for the samples A2–D2 immersed in distilled water, at 36.5°C, for 21 days. The values are increasing with the CA content in the scaffolds

The X-ray microanalysis identified calcium and phosphorus in the mineralized structures with a Ca/P ration of 1.53. This information, correlated with the morphology of the calcified structure corresponds to CDHA (occasionally named precipitated HA). The X-ray Ca and P evaluation of the hydrogels has been performed. The microanalysis proved that Ca and P atoms have distinguished from the C and O characteristic for the polymer matrix only in the thick mineral deposits. Cl has also been detected, probably resulted from the residual sodium chloride very difficult to remove after the incubation in SBF. These results suggest that only samples A2 and B2 were able to form extensive CDHA deposits onto their surface following the incubation in SBF. The hydrogels C2 and D2 have only shown apatite nucleation areas embedded in the polymer matrix, without well identified CDHA layer-like formation.

FT-IR spectra have successfully proved the formation of phosphate-containing mineral following the incubation in SBF. As it is well known, typical apatite presents OH^- stretching vibration at 3570 cm^{-1} and PO_4^{3-} vibration modes at 1096, 1036 and at 960 cm^{-1}, respectively. Additionally, carbonated apatite present, besides the phosphate vibrations, carbonate vibrations at about 1400 cm^{-1} ($\nu 3$) and at 870 cm^{-1}($\nu 2$), respectively [17–19]. Before incubation all the polymers have presented typical O–H and N–H vibrations at about 3300–3400 cm^{-1}, due to the abundance of such groups in the Gel and alginate components. Amide I and II (at 1630 and 1545 cm^{-1}, respectively) are also visible due to the peptide. All these peaks are, as expected, still visible even after the SBF immersion. However, very important spectral differences might be noticed after the SBF treatment. All the SBF-immersed hydrogels have presented typical phosphate vibrations in the 1000–1100 cm^{-1} wavenumber range. Very important, spectral differences are visible as follows.

The samples A2 and B2 corresponding to the substrates with a lower CA content presented PO_4^{3-} vibration bands in the range of 1100–1000 cm^{-1} and at about 945 cm^{-1}. A shift of the OH^- stretching vibration from approximately 3282 cm^{-1} (before incubation) to 3371 cm^{-1} following SBF-immersion is probably due to the OH^- stretching vibration from the mineral phase. On the other hand, the samples C2 and D2 (with higher CA content) presented, besides phosphate vibrations, carbonate-specific peaks at about 1400 cm^{-1} and at 822 cm^{-1}. The OH^- stretching vibration (due to the mineral formed after the mineralization test) does not distinguish anymore from the spectra of the hydrogels; this fact may be due to a hydroxyl partial replacement by carbonate ions. It can be concluded that

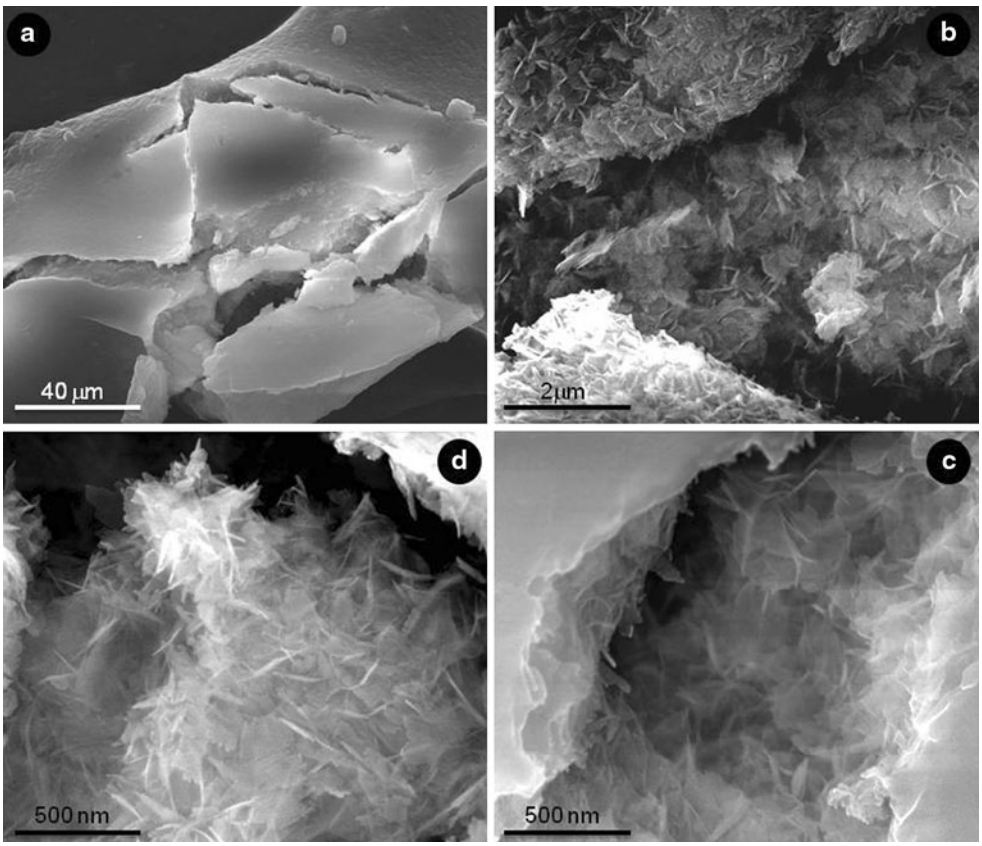

Fig. 6 Morphology of the mineral deposits formed onto Gel-CA hydrogels incubated in SBF for 3 weeks, as obtained by SEM. **a**, **b** morphology of the mineral formed on A2, with elementary features consisting in small tablets and needle-like entities; **c**, **d** mineral structure formed on the surface of B2-small tablets (approximately 100 nm long and 10 nm width) and needle-like aspect

FT-IR spectra bring significant evidence for the presence of mineral phase after the incubation of materials. Moreover, IR analysis provided important spectroscopic proofs to distinguish between the two types of mineral corresponding to different scaffolds. Apatite mineral has bee found only in samples A2 and B2. Even the nucleation noticed through SEM on C2 and D2 has been detected by FT-IR; the analysis indicated the formation of carbonated apatite.

Gel-CA-based compositions were investigated in different works for different biomedical applications ranging from controlled delivery [20, 21] to wound dressing [22, 23] and control of the mineral phase morphology [24]. However, the systems developed in this work are obtained through a different method previously described.

Gel was selected due to its collagenic origin. The modulation of calcium phosphates formation in different calcification systems based on Gel has been previously reported [6, 7, 24–26]. However, to the best of our knowledge none of these works referred to the ability of Gel scaffolds to induce biomimetic mineralization when immersed in simple SBF; their suitability to evaluate the effects of mineralization-related proteins on calcium phosphate nucleation and growth has been explored. Nevertheless, the methods used mainly consisted in the diffusion of calcium and phosphate solutions of variable characteristics (pH, concentration) through Gel-based conventional or double diffusion systems [6, 7, 25], in the synthesis of HA with controlled morphology through simultaneous titration of calcium chloride, sodium dibasic phosphate and Gel-SA solution [24] or in the biomimetic mineralization when porous 3D Gel was immersed for several days in 1.5× SBF [26].

Although CA is not directly related to hard tissues, it was used due to its calcium content and also because it could serve as a reference in assessing the role of glycosylated molecules in the biomineralization occurrence. On the other hand, starting from the demonstrated capacity of carboxyl-rich organic polymer gels to induce calcification, the apatite-forming ability of CA has been investigated [27]. The material may induce apatite formation in SBF but only after extensive $Ca(OH)_2$ treatment [27]. Nevertheless, the apatite-deposition on other polysaccharides has been associated with extensive residual $CaCl_2$ in the studied polymer, leading to calcium release in the SBF followed by an increase of the calcium concentration and an increase of the free carboxylates with high affinity towards calcium

ions [5]. Basically, the free carboxylates behave like the driving force responsible for calcium phosphates nucleation and eventual growth, but only if the matrix is previously loaded with calcium containing species ($Ca(OH)_2$, $CaCl_2$) [5, 27]. It was also demonstrated that the addition of CA strongly influences the structure and morphology of HA-Gel composites [24].

In this context, our study has proved the ability of CA combined with crosslinked Gel to promote apatite-like mineral formation under in vitro biomimetic conditions, only for the compositions corresponding to 100/2 and 100/4 (wt/wt) Gel:SA. This implies that increasing the CA concentration above a certain threshold (in this study compositions with Gel:SA in the range of 100:4–100:8 (wt/wt)) leads to probably too many calcium carboxylates efficient to induce nucleation but not the growth of the apatite crystals. In this context, it is important to eliminate the hypothesis of a simple positive influence of the $CaCl_2$ crosslinking agent on the occurrence of the CDHA formation on the interpenetrated Gel-CA materials studied here. This effect has been carefully avoided through the extensive water extraction of the residual $CaCl_2$.

Thus, it seems that apatite formation was enhanced by the porosity of the materials and by the intrinsic 3D structure of the hydrogels; the presence of CA in the Gel-based materials definitely favored the calcification occurrence. CA is responsible for intermolecular interactions with the peptide and, depending on its concentration in the organic insoluble matrix, it could enhance the mineralization occurrence under biomimetic conditions. However, the mineralization-promoting effect of the peptide-polysaccharide interconnected network strictly depends on the hydrogels structural, compositional and morphological features derived from the interaction between the two components.

5 Conclusions

The present study suggests that a convenient porous structure of an already intrinsically 3D organized Gel hydrogel, complemented with a controlled amount of CA, could be beneficial in inducing a biomimetic spontaneous mineralization. Further work should be devoted to the optimization of these materials. Despite the modest biomechanical performances (not discussed here) of these biopolymer scaffolds, the hydrogels present potential for complex formulation to be used in load-bearing biomedical applications. In this respect, further studies are in progress to better control the factors deciding the mineralization occurrence.

Acknowledgments The National Authority for Scientific Research from The Ministry of Education, Research and Youth of Romania is gratefully acknowledged for the financial support through the Human Resources project study of the biomimetic mineralization using specifically functionalized 3D hydrogels, PN-II-RU-TE-2009-10, code TE_80.

References

1. Dorozhkin SV. Nanosized and nanocrystalline calcium orthophosphates. Acta Biomater. 2010;6(3):715–34.
2. Dorozhkin SV. Bioceramics of calcium orthophosphates. Biomaterials. 2010;31:1465–85.
3. Dorozhkin SV. Calcium orthophosphate-based biocomposites and hybrid biomaterials. J Mater Sci. 2009;44:2343–87.
4. Garnett J, Dieppe P. The effects of serum and human albumin on calcium hydroxyapatite crystal growth. Biochem J. 1990;266:863–8.
5. Munarin F, Giuliano L, Bozzini S, Tanzi MC, Petrini P. Mineral phase deposition on pectin microspheres. Mater Sci Eng C. 2010;30:491–6.
6. Teng S, Shi J, Chen L. Formation of calcium phosphates in gelatin with a novel diffusion system. Colloids Surf B Biointerf. 2006;49:87–92.
7. Wen HB, Moradian-Oldak J, Fincham AG. Dose-dependent modulation of octacalcium phosphate crystal habit by amelogenins. J Dent Res. 2000;79:1902–6.
8. Tampieri A, Celotti G, Landi E. From biomimetic apatites to biologically inspired composites. Anal Bioanal Chem. 2005;381:568–76.
9. Kamei I, Tomita N, Tamai S, Kato K, Ikada Y. Histologic and mechanical evaluation for bone bonding of polymer surfaces grafted with a phosphate-containing polymer. J Biomed Mater Res. 1997;37:384–93.
10. Shin H, Jo S, Mikos AG. Biomimetic materials for tissue engineering. Biomaterials. 2003;24:4353–64.
11. Stancu IC, Filmon R, Cincu C, Marculescu B, Zaharia C, Tourmen Y, Baslé MF, Chappard D. Synthesis of methacryloyloxyethyl phosphate copolymers and in vitro calcification capacity. Biomaterials. 2004;25:205–13.
12. Vallet-Regí M, González-Calbet JM. Calcium phosphates as substitution of bone tissues. Progr Solid St Chem. 2004;32:1–31.
13. Weiner S, Addadi L. Design strategies in mineralized biological materials. J Mater Chem. 1997;7:689–702.
14. Weiner S, Wagner HD. The material bone: structure mechanical function relations. Annu Rev Mater Sci. 1998;28:271–98.
15. Mann S. Biomineralization. Principles and concepts in bioinorganic materials chemistry. New York: Oxford University Press; 2001.
16. Kokubo T, Takadama H. How useful is SBF in predicting in vivo bone bioactivity? Biomaterials. 2006;27(15):2907–15.
17. Mihailova B, Kolev B, Balarew C, Dyulgerova E, Konstantivov L. Vibration spectroscopy study of hydrolyzed precursors for sintering calcium phosphate bio-ceramics. J Mater Sci. 2001;36:4291–7.
18. Honda Y, Kamakura S, Sasaki K, Suzuki O. Formation of bone-like apatite enhanced by hydrolysis of octacalcium phosphate crystals deposited in collagen matrix. J Biomed Mater Res Part B Appl Biomater. 2007;80B:281–9.
19. Habibovic P, Juhl MV, Clyens S, Martinetti R, Dolcini L, Theilgaard N, van Blitterswijk CA. Comparison of two carbonated apatite ceramics in vivo. Acta Biomater. 2010;6:2219–26.

20. Ferreira Almeida P, Almeida AJ. Cross-linked alginate–gelatine beads: a new matrix for controlled release of pindolol. J Control Rel. 2004;97(3):431–9.
21. Dong Z, Wang Q, Du Y. Alginate/gelatin blend films and their properties for drug controlled release. J Membr Sci. 2006;280: 37–44.
22. Balakrishnan B, Mohanty M, Umashankar PR, Jayakrishnan A. Evaluation of an in situ forming hydrogel wound dressing based on oxidized alginate and gelatin. Biomaterials. 2005;26:6335–42.
23. Choi YS, Hong SR, Lee YM, Song KW, Park MH, Nam YS. Study on gelatin-containing artificial skin: I. Preparation and characteristics of novel gelatin-alginate sponge. Biomaterials. 1999;20:409–17.
24. Teng S, Shi J, Peng B, Chen L. The effect of alginate addition on the structure and morphology of hydroxyapatite/gelatin nanocomposites. Compos Sci Technol. 2006;66:1532–8.
25. Boskey A. Hydroxyapatite formation in a dynamic collagen gel system: effects of type I collagen, lipids, and proteoglycans. J Phys Chem. 1989;93(4):1628–33.
26. Liu X, Smith LA, Hu J, Ma PX. Biomimetic nanofibrous gelatin/apatite composite scaffolds for bone tissue engineering. Biomaterials. 2009;30:2252–8.
27. Kokubo T, Hanakawa M, Kawashita M, Minoda M, Beppu T, Miyamoto T, Nakamura T. Apatite deposition on calcium alginate fibres in simulated body fluid. J Ceram Soc Jpn. 2004;112: 363–7.